A Numerical Investigation of the Effect of Electric Charges and Vertical External Electric Fields on the Collision Efficiency of Cloud Drops: Part II

R. J. SCHLAMP, S. N. GROVER AND H. R. PRUPPACHER

Department of Atmospheric Sciences, University of California at Los Angeles, 90024

A. E. HAMIELEC

Department of Chemical Engineering, McMaster University, Hamilton, Ontario Canada L8S-4K1

(Manuscript received 21 July 1978, in final form 10 October 1978)

ABSTRACT

The numerical model of Schlamp *et al.* (1976) for determining the collision efficiency of electrically charged or uncharged cloud drops in the presence or absence of a vertical electric field has been extended to study the two following cases, both of which include the presence of a vertical field due to a net positive charge in the upper part of the cloud and a net negative charge in the lower part of the cloud: (i) the larger drop is negatively charged and is initially above the smaller drop, which is positively charged; (ii) the larger drop is negatively charged and it is initially *below* the smaller drop, which is again positively charged. Also, for the purpose of resolving more accurately the critical electric charge on the drops and the critical electric field necessary to significantly affect the collision efficiency, additional computations have been carried out for charged drops in the absence of an electric field and for uncharged drops in the presence of a vertical electric field.

The sizes of drops considered range from 1–118 μm in radius. The magnitude of the electric charges on the drops range from 0–2.8×10^{-4} esu, and the electric fields range in strength from 0–3429 V cm^{-1}, which include the charges and fields typically observed in thunderstorms.

It is found that electric fields and charges even of relatively modest values have a profound effect upon the collision efficiency. The results of case (i) show that the electrostatic forces are responsible for determining the shape of the collision efficiency curves with the hydrodynamic forces being of secondary importance. These results are significantly different from either those of case (ii) or those of Schlamp *et al.* (1976).

1. Introduction

In a recent article (Schlamp *et al.*, 1976) we presented a numerical investigation on the effects of electrical charges and vertical external electric fields on the collision efficiency of spherical water drops falling in air. In that study the vertical electrical field was assumed to be downward pointing (negative) due to a net positive charge in the upper part of the cloud and a net negative charge in the lower part of the cloud. The larger A drop was assumed to be positively charged and was initially above the smaller a drop, which was negatively charged. For these conditions, the efficiency E with which an A drop collides with an a drop, was numerically determined. The results were summarized in seven diagrams in which E versus a was graphed for $A=11.4$, 19.5, 31.4, 40.2, 50.7, 61.7 and 74.3 μm. The sizes of the a drops considered varied from 1 to 66 μm. The magnitude of the electric charges on the drops ranged from 0–1.1×10^{-4} esu,[1] and the external electric fields ranged in strength from 0–3429 V cm^{-1}, which included the charges and fields typically observed in thunderstorms.

During the review process of that article, as well as during its presentation at the International Cloud Physics Conference in Boulder during August 1976, it was pointed out by various scientists that it seemed highly desirable to extend the study of Schlamp *et al.* (1976) to include the case where the A drop is *negatively* charged and the a drop *positively* charged in a downward pointing external electric field. Such a study appeared justifiable from the following: A switch in the choice of sign for the electric charge on the drops while maintaining the same external field orientation produces an electrostatic force on each drop significantly different in magnitude and direction due to charge and field interactions. Further, the drops' initial relative velocity and thus their interaction time is importantly altered.

[1] Since the theoretical results of Davis (1964a), given in the form of complicated analytic expressions and a large number of tables, have been expressed in electrostatic units, and since the results are an integral part of our computations, we have in several places in our paper used electrostatic units rather than the AMS recommended SI units.

0022-4928/79/020339-11$06.75

These effects are expected to produce values for the collision efficiency considerably different from those of Schlamp *et al.* (1976).

Motivated by this reasoning, we have undertaken a series of new computations using the theoretical model and computational scheme of Schlamp *et al.* Since the physics and mathematics of this model has been described in detail in this earlier paper, it shall not be repeated here. It shall merely be mentioned that the new calculations were again carried out for environmental conditions of 800 mb and +10°C for the A drop parameters listed in Table 1. The computational procedure required an accurate description for flow about each drop. For drops with $0.02 \leqslant N_{\mathrm{Re}} \leqslant 10.0$ we used flow fields numerically given by LeClair *et al.*, (1970) and for drops of $N_{\mathrm{Re}} < 0.02$ we assumed the flow field was given by Proudman and Pearson's (1957) analytic solution to the Navier–Stokes equations of motion. Thus, in all cases studied the hydrodynamic drag forces used are a result of the superpositioning of the flow fields about each of the two interacting drops.

For the purpose of describing the electrostatic forces acting on each of the interacting drops, we used the model of Davis (1962, 1964a, b) who represented both drops by conducting spheres. Written in slightly different notation than in Schlamp *et al.* (1976), we find for the nondimensional electrostatic force $\mathbf{F}'_{e,a}$ on the a drop[2]

$$\begin{aligned}\mathbf{F}'_{e,a} = &-(\tfrac{3}{4}\pi V^2_{\infty,A})[\epsilon p^2 E_0^2 (F_1 \cos^2\gamma + F_2 \sin^2\gamma) \\ &+ E_0 q_A \cos\gamma (F_3 - p^2 F_4) + q_A^2 \epsilon^{-1} (F_5 p^{-2} - F_6 + p^2 F_7) \\ &- E_0 q_A p^2 \cos\gamma]\mathbf{e}_r + (\tfrac{3}{4}\pi V^2_{\infty,A})[\epsilon p^2 E_0^2 F_8 \sin 2\gamma \\ &+ E_0 q_A \sin\gamma (F_9 - p^2 F_{10}) - E_0 q_A p^2 \sin\gamma]\mathbf{e}_\gamma, \quad (1)\end{aligned}$$

where γ is the angle between the local vertical, given by the direction of gravity, and the line connecting the centers of the interacting drops,[3] and $p = a/A$. The nondimensional electrostatic force $\mathbf{F}'_{e,A}$ on the A drop is then given as

$$\mathbf{F}'_{e,A} = (\tfrac{3}{4}\pi V^2_{\infty,A})[\mathbf{E}_0 q_A (1 - p^2) - (\mathbf{F}_{e,a}/A^2)]. \quad (2)$$

It must be stressed that in the present set of computations the electric charge on each of the drops was again calculated according to the relations $q_A = Q_A/A^2 = \pm C$, $q_a = Q_a/a^2 = \mp C$, and therefore, $q_a = -q_A$, where charge is expressed in electrostatic units and drop radius in centimeters. These expressions result from observations

TABLE 1. Combinations of collector drop radius, terminal velocity, Reynolds number and electric force used in the present work.

A (μm)	$V_{\infty,A}$ (cm s^{-1})	$N_{\mathrm{Re},A}$	$Q_A E_0$ (C V m^{-1})
11.4	1.59	0.02	0.0
11.4	3.17	0.04	-6.1×10^{-11}
11.4	7.94	0.1	-2.5×10^{-10}
19.5	3.23	0.07	$+9.3\times10^{-11}$
19.5	4.62	0.1	0.0
19.5	9.24	0.2	-3.1×10^{-10}
19.5	13.86	0.3	-6.3×10^{-10}
31.4	5.74	0.2	$+6.5\times10^{-10}$
31.4	8.61	0.3	$+3.3\times10^{-10}$
31.4	17.23	0.6	-6.8×10^{-10}
31.4	28.71	1.0	-2.1×10^{-9}
40.2	4.49	0.2	$+2.0\times10^{-9}$
40.2	13.46	0.6	$+7.1\times10^{-10}$
40.2	22.44	1.0	-7.4×10^{-10}
40.2	39.27	1.75	-3.7×10^{-9}
50.7	10.68	0.6	$+3.4\times10^{-9}$
50.7	17.80	1.0	$+1.9\times10^{-9}$
50.7	35.60	2.0	-2.1×10^{-9}
50.7	44.50	2.5	-4.3×10^{-9}
61.7	21.96	1.5	$+4.3\times10^{-9}$
61.7	29.29	2.0	$+2.2\times10^{-9}$
61.7	43.93	3.0	-2.3×10^{-9}
61.7	58.57	4.0	-7.2×10^{-9}
74.3	30.38	2.5	$+7.2\times10^{-9}$
74.3	42.53	3.5	$+2.5\times10^{-9}$
74.3	54.69	4.5	-2.6×10^{-9}
74.3	72.91	6.0	-1.1×10^{-8}

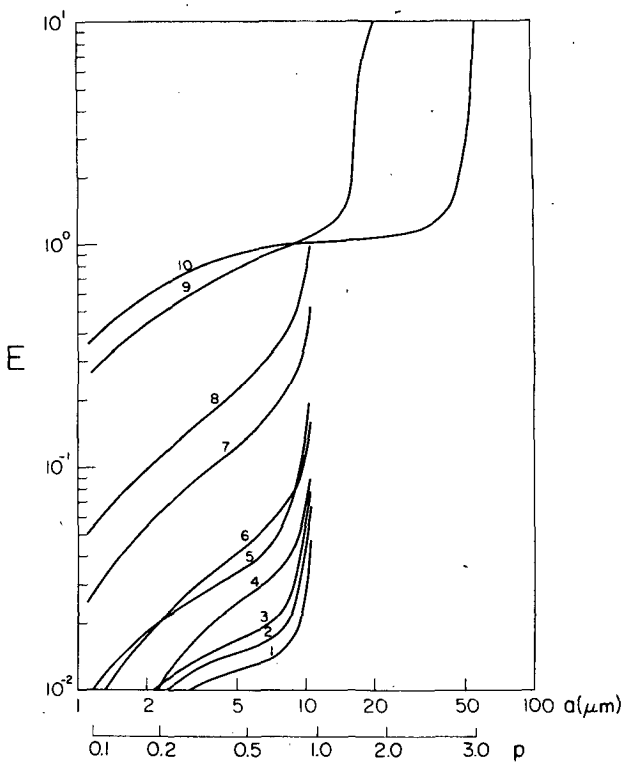

FIG. 1. Present results for the efficiency with which a cloud drop of radius $A = 11.4$ μm collides with cloud drops of radius a where $p = a/A$.

[2] The symbols appearing in this and subsequent equations are the same as those of Schlamp *et al.* (1976).

[3] Note that in our previous article (Schlamp *et al.*, 1976) Eq. (12) which corresponds to the present Eq. (1) is erroneous in that the last term on the right side of Eq. (12) should read $E_0 Q_a \sin\gamma$.

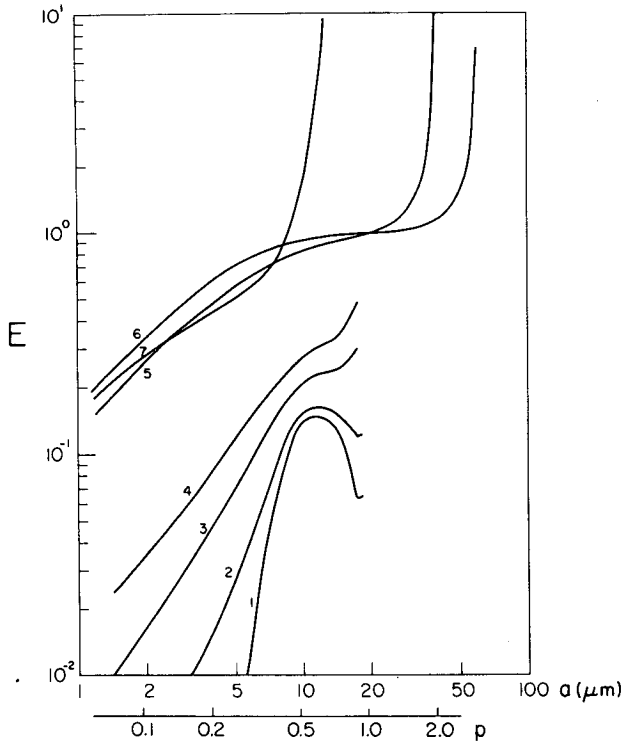

FIG. 2. As in Fig. 1 except for $A = 19.5\ \mu$m.

summarized by Takahashi (1972, 1973), where the constant $C = 2$ represents a mean drop charge in thunderstorms.

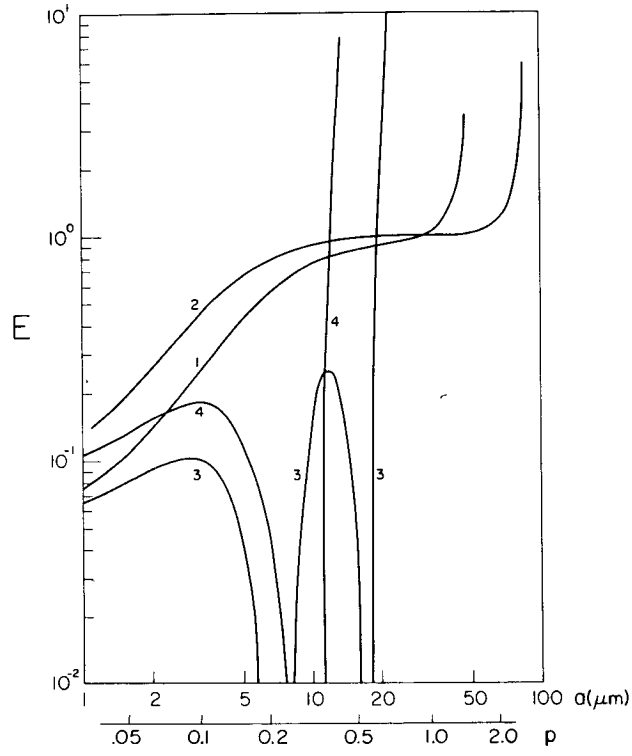

FIG. 3. As in Fig. 1 except for $A = 31.4\ \mu$m.

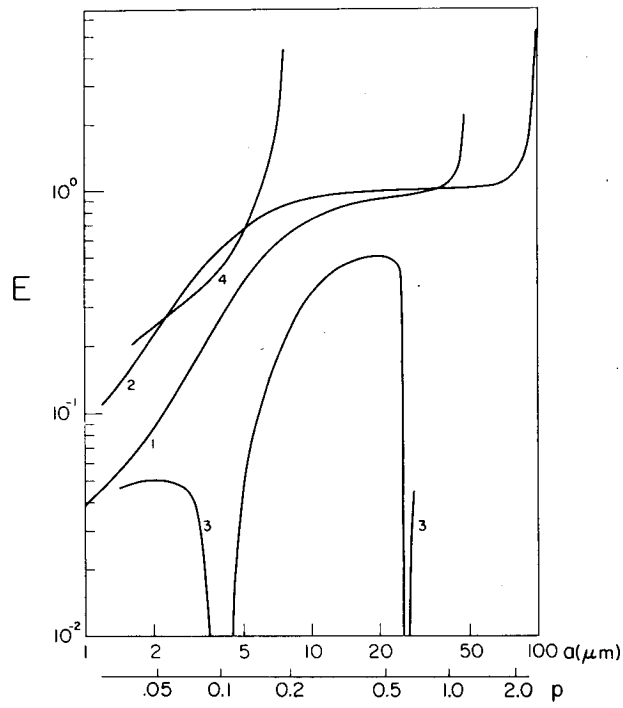

FIG. 4. As in Fig. 1 except for $A = 40.2\ \mu$m.

The new study examined the two following cases, both of which include the presence of a downward pointing external electric field:

(i) The larger drop is negatively charged and is initially above the smaller drop, which is positively charged.

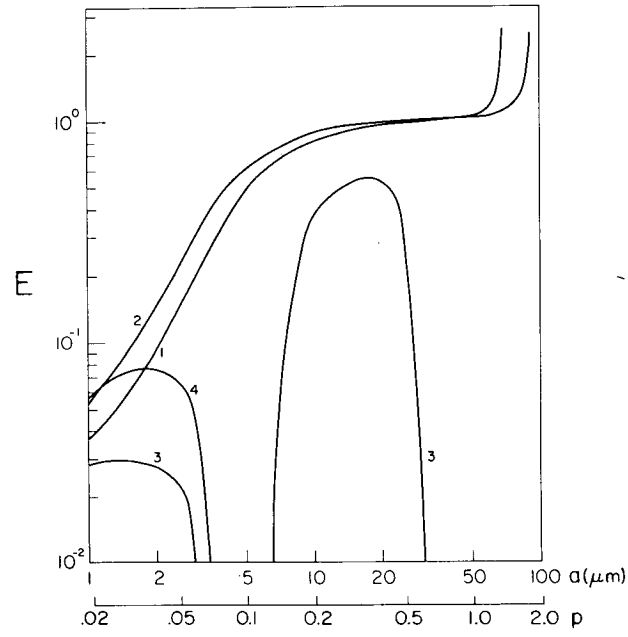

FIG. 5. As in Fig. 1 except for $A = 50.7\ \mu$m.

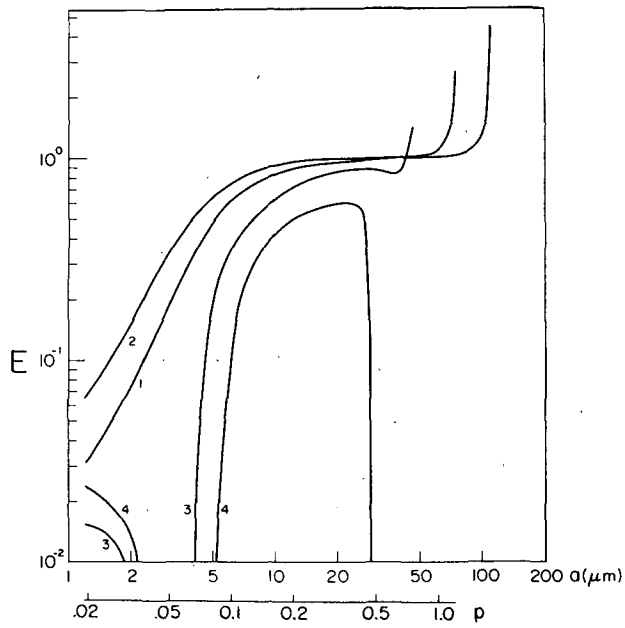

FIG. 6. As in Fig. 1 except for $A = 61.7$ μm.

(ii) The larger drop is negatively charged and is initially *below* the smaller drop, which is again positively charged. These latter computations were carried out in order to extend the computations of Schlamp *et al.* (1976) to larger radii of the a drop. Also, for the purpose of resolving more accurately the critical electric charge on the drops and the critical electric field necessary to significantly affect the collision efficiency, additional computations for charged drops in the absence of an electric field and for uncharged drops in the presence of a vertical electric field have been carried out.

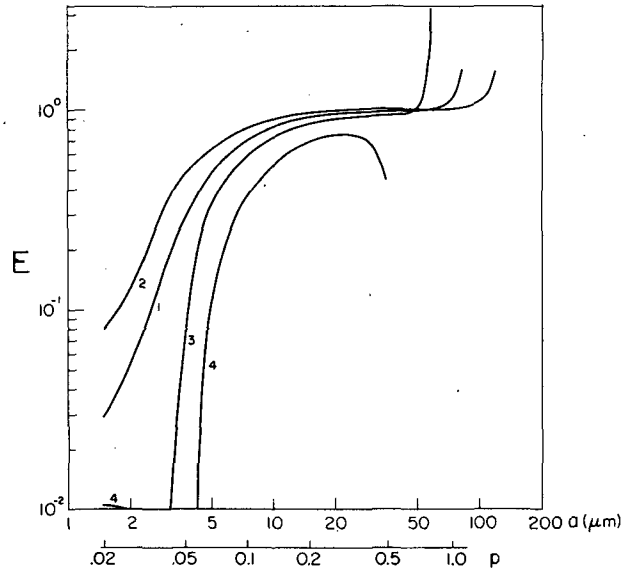

FIG. 7. As in Fig. 1 except for $A = 74.3$ μm.

TABLE 2a. Legend for curves in Fig. 1. Multiply electric field by 100 to convert to volts per meter

$A = 11.4$ μm curve	q_A (esu cm^{-2})	q_a (esu cm^{-2})	E_0 (V cm^{-1})
1	0	0	0
2	±0.05	∓0.05	0
3	±0.075	∓0.075	0
4	0	0	±50
5	±0.2	∓0.2	0
6	0	0	∓100
7	0	0	∓300
8	0	0	∓500
9	±2.0	∓2.0	∓706
10	±2.0	∓2.0	∓2847

TABLE 2b. As in Table 2a except for Fig. 2

$A = 19.5$ μm curve	q_A (esu cm^{-2})	q_a (esu cm^{-2})	E_0 (V cm^{-1})
1	0	0	0
2	0	0	∓100
3	0	0	∓300
4	0	0	∓500
5	±2.0	∓2.0	∓1236
6	±2.0	∓2.0	∓2504
7	∓2.0	±2.0	∓ 364

TABLE 2c. As in Table 2a except for Fig. 3

$A = 31.4$ μm curve	q_A (esu cm^{-2})	q_a (esu cm^{-2})	E_0 (V cm^{-1})
1	±2.0	∓2.0	∓1038
2	±2.0	∓2.0	∓3234
3	∓2.0	±2.0	∓502
4	∓2.0	±2.0	∓992

TABLE 2d. As in Table 2a except for Fig. 4

$A = 40.2$ μm curve	q_A (esu cm^{-2})	q_a (esu cm^{-2})	E_0 (V cm^{-1})
1	±2.0	∓2.0	±683
2	±2.0	∓2.0	∓3529
3	∓2.0	±2.0	∓ 659
4	∓2.0	±2.0	∓1899

TABLE 2e. As in Table 2a except for Fig. 5.

$A = 50.7$ μm curve	q_A (esu cm^{-2})	q_a (esu cm^{-2})	E_0 (V cm^{-1})
1	±2.0	∓2.0	∓1208
2	±2.0	∓2.0	∓2485
3	∓2.0	±2.0	∓1133
4	∓2.0	±2.0	∓1977

TABLE 2f. As in Table 2a except for Fig. 6.

$A=61.7$ μm curve	q_A (esu cm^{-2})	q_a (esu cm^{-2})	E_0 (V cm^{-1})
1	±2.0	∓2.0	∓907
2	±2.0	∓2.0	∓2842
3	∓2.0	±2.0	∓846
4	∓2.0	±2.0	∓1682

TABLE 2g. As in Table 2a except for Fig. 7

$A=74.3$ μm curve	q_A (esu cm^{-2})	q_a (esu cm^{-2})	E_0 (V cm^{-1})
1	±2.0	∓2.0	∓705
2	±2.0	∓2.0	∓2960
3	∓2.0	±2.0	∓680
4	∓2.0	±2.0	∓1957

2. Results and discussion

Collision efficiencies were again computed for collector drop radii $11.4 \leqslant A \leqslant 74.3$ μm and collected drop radii $1 \leqslant a \leqslant 128$ μm. Summarized in Figs. 1–7 are the present results for E for various field and charge combinations with the numbered curves identified in Tables 2a–2g. In confirmation of the findings of Schlamp *et al.* (1976), the present results allow the following conclusions:

1) External electric fields E_0 as well as electric charges Q residing on the interacting cloud drops may have a profound effect on the efficiency with which these drops collide. In fact, under thunderstorm conditions the collision efficiency E may be raised up to two orders of magnitude.

2) External electric fields in the presence of electrically neutral drops invariably enhance the collision efficiency of the drops with the enhancement most pronounced for the smallest A drops.

3) In the absence of an external electric field, electric charges of opposite sign residing on drops invariably raise the collision efficiency of the drops with the increase most pronounced for the smallest A drops.

4) The influence of the electrostatic effects described above decreases with increasing A-drop radius becoming negligible for $\gtrsim 70$ μm, even in the presence of the highest electric fields and charges observed in clouds.

5) For a given A drop radius, the enhancement of E due to either electric charges or an external electric field depends on the size ratio $p=a/A$. This effect is largest for $p \gg 1$, least for intermediate p and increases again as $p \approx 1$.

Conclusions 1–3 are in qualitative agreement with the analytical studies of Sartor (1960), Davis (1965) and Krasnogorskaya (1965) who assumed two-body Stokes flow around a falling drop, and with the analytical studies of Lindblad and Semonin (1963), Plumlee and Semonin (1965) and Semonin and Plumlee (1966) who assumed that the flow about a drop could be approximated by Proudman and Pearson's analytic expression. Conclusions 1–4 also are in qualitative agreement with the results of Sartor (1970) who computed drop trajectories using the results of Davis (1964a,b) for the electric forces on a 10 and 30 μm radius collector drop in two-body Stokes flow, for a 100 μm radius collector drop in single-body Stokes flow acted on by an empirically derived drag, and for 1000 μm radius collector drops in potential flow acted on by an empirically derived drag. In Sartor's study the drops either carried high opposing electric charges (10 A^2 esu) or were uncharged but exposed to a high external electric field (3000 V cm^{-1}). Conclusions 1 and 2 are in qualitative agreement also with the results of Atkinson and Paluch (1968) and Paluch (1970) who developed an analytical model which determines the collision efficiency of highly charged drops in Stokes flow under the assumption that the drops have negligible inertia and undergo negligible hydrodynamic interaction such that the Stokes drag on each drop just balances the applied forces from gravity, from Coulomb interaction and from the external electric field.

Although the studies mentioned are in qualitative agreement with our findings they fail to give quantitative agreement due to their approximate description of the flow past the interacting drops and/or due to their simplified description of the electric forces between the drops. In addition, the model of Atkinson and Paluch (1968) and Paluch (1970) only applies to drops carrying unrealistically large charges as verified experimentally by Abbott (1975) and Krasnogorskaya and Neizvestnyy (1973).

In addition to confirming the results of Schlamp *et al.* (1976), the *new calculations* allow the following additional conclusions:

1) In the *absence of electric charges* on the drops, the collision efficiency may be raised by more than a few percent if $E_0 \gtrsim 25$–50 V cm^{-1} for $A \approx 10$ μm, $E_0 \gtrsim 50$–100 V cm^{-1} for $A \approx 20$ μm, $E_0 \gtrsim 100$–500 V cm^{-1} for $A \approx 30$ μm and $E_0 \gtrsim 500$–1000 V cm^{-1} for $A \approx 40$ μm. In the *absence of an external electric field*, the collision efficiency may be raised by more than a few percent if $Q_A \gtrsim 5\times10^{-8}$ esu for $A \approx 10$ μm, $Q_A \gtrsim 10^{-6}$ esu for $A \approx 20$ μm and $Q_A \gtrsim 5\times10^{-5}$ esu for $A \approx 40$ μm. These results show that the critical parameter necessary to affect the collision efficiency increases with increasing A drop radius for uncharged drops in the presence of an external electric field or for charged drops in the absence of an electric field. These new findings are in qualitative agreement with the findings of Sartor (1960), Lindblad and Semonin (1963), Plumlee and Semonin (1965), Davis (1965), Krasnogorskaya (1965) and Semonin and Plumlee (1966).

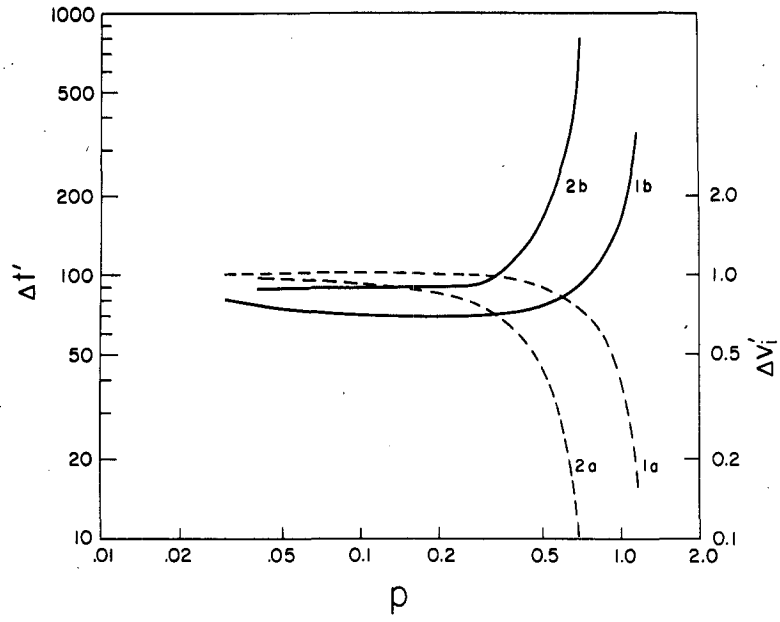

FIG. 8. Nondimensional initial relative velocity (curves a) and nondimensional trajectory interaction time (curves b) as a function of $p=a/A$ for two drops aerodynamically interacting: 1) $A=40.2$ μm, $q_A=+2=-q_a$, $E_0=682$ V cm^{-1}; 2) $A=40.2$ μm, $q_A=-2=-q_a$, $E_0=659$ V cm^{-1}.

2) In the *presence of a downward pointing electric field*, considerable differences are found in E vs a (or E vs p) for a *positively* charged A drop and a *negatively* charged a drop, and for the case where the electric charge signs are reversed. Thus, for a given radius of the A drop, for a given magnitude of the external electric field and for $q_A=+2=-q_a$, the collision efficiency generally increases with increasing a drop radius. This behavior is readily understandable from the following: The initial rise of E with p is characterized by a large initial vertical component of the relative velocity of the two drops which gives rise to relatively short interaction times. This is illustrated for a 40.2 μm radius A drop by curves 1a and 1b in Fig. 8. Increasing a drop inertia in the p ratio range $p\lesssim 0.2$ results in a decreasing ability of the a drop to avoid collision with the larger A drop. This is followed by a wide range of p within with E is near the geometric value. Eventually, the radius of the a drop exceeds a certain critical value, which quite strongly depends on the external electric field strength and on the electric charges on the a drop, to provide a much decreased initial relative vertical velocity and therefore increased interaction time, as illustrated in Fig. 8. Then the a drop's increasingly vigorous hydrodynamic wake has sufficient time to act on the A drop to cause a second rise in E with p.

For all values of p, the electrostatic forces act to bring both drops together during the entire length of their trajectories. As p increases from its lower to its higher value the nondimensional electrostatic forces on the a drop increase in strength up to two orders of magnitude. The overall result is to enhance the collision efficiency of each A drop considered, especially for the smallest a drop with least inertia and for the largest a drop with the most vigorous wake.

3) However, if in a downward pointing electric field a *negatively* charged A drop interacts with a *positively* charged a drop, the collisional behavior becomes unexpectedly complex. A careful analysis of the trajectories of colliding drops reveals that in some cases collisions were found to occur both on the A drop's front *and* rear hemispheres, or on the A drop's rear hemisphere only. Such behavior is in contrast to the previously discussed case (ii) of reversed electric sign where only collisions with the A drop's front hemisphere were observed to take place.

The complicated nature of this behavior becomes clarified if for each A drop E is split into a front collision efficiency E_{Front} and a rear collision efficiency E_{Rear} such that $E=E_{\text{Front}}+E_{\text{Rear}}$. Figs. 9 and 10 present these collision efficiencies versus p for low electric field values for the various A drop radii, where the numbered curves are identified in Table 3.

In an attempt to explain the various maxima and minima seen in these figures, especially for E_{Rear}, we looked in particular at the case $A=40.2$ μm, $q_A=-2=-q_a$ and $E_0=-659$ V cm^{-1} for which E versus p is displayed by curves 3 in Figs. 4, 9 and 10. The 40.2 μm A drop was chosen for the following two reasons: First, this size lies basically in the middle of the range of collector sizes considered. Second, this A drop exhibited solely rear collisions at the lowest

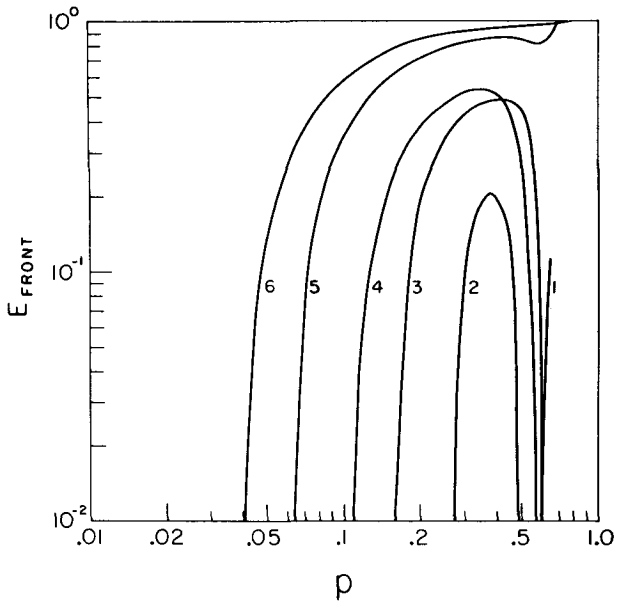

FIG. 9. Present results for E_{Front} (as defined in the text) for each A drop as a function of $p=a/A$ for low electric field values.

and highest p ratios, mainly front collisions at intermediate values of p, and two regions of *zero* collisions near $p=0.1$ and $p=0.65$. Since this type of behavior

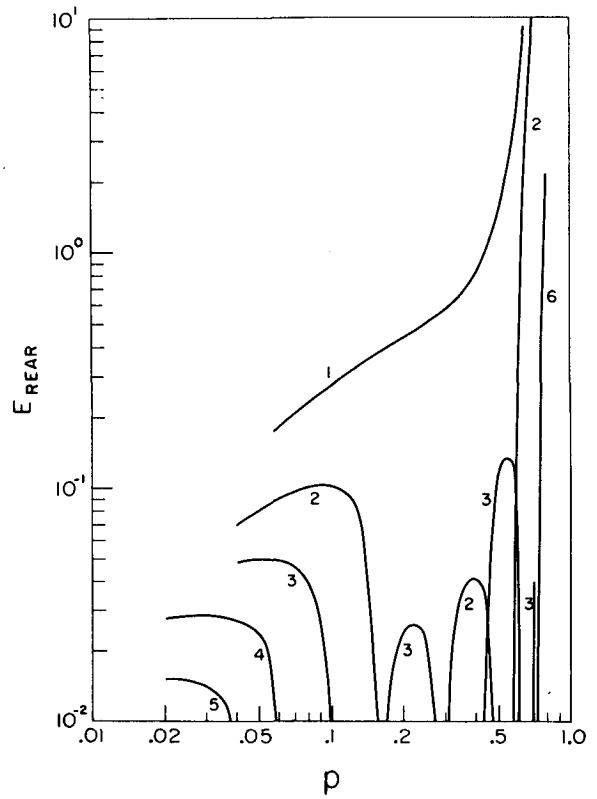

FIG. 10. Present results for E_{Rear} (as defined in the text) for each A drop as a function of $p=a/A$ for low electric field values.

TABLE 3. Legend for curves in Figs. 9 and 10. Multiply electric field by 100 to convert to volts per meter.

Curve	A (μm)	q_A (esu cm^{-2})	q_a (esu cm^{-2})	E_0 (V cm^{-1})
1	19.5	$\mp$2.0	$\pm$2.0	$\mp$364
2	31.4	$\mp$2.0	$\pm$2.0	$\mp$502
3	40.2	$\mp$2.0	$\pm$2.0	$\mp$659
4	50.7	$\mp$2.0	$\pm$2.0	$\mp$1133
5	61.7	$\mp$2.0	$\pm$2.0	$\mp$846
6	74.3	$\mp$2.0	$\pm$2.0	$\mp$680

is typical of many of the A drops the conclusions derived for this collector drop size could be applicable to all of the results.

In looking at the behavior of the 40.2 μm drop, Figs. 9 and 10 show (curves 3) that for $p<0.1$, only rear collisions occurred. These interactions are typified by the trajectories displayed in Fig. 11 for $A=40.2$ μm, $a=2.4$ μm and $p=0.06$. The trajectory labeled Crit in this (and all following) figures is the grazing tra-

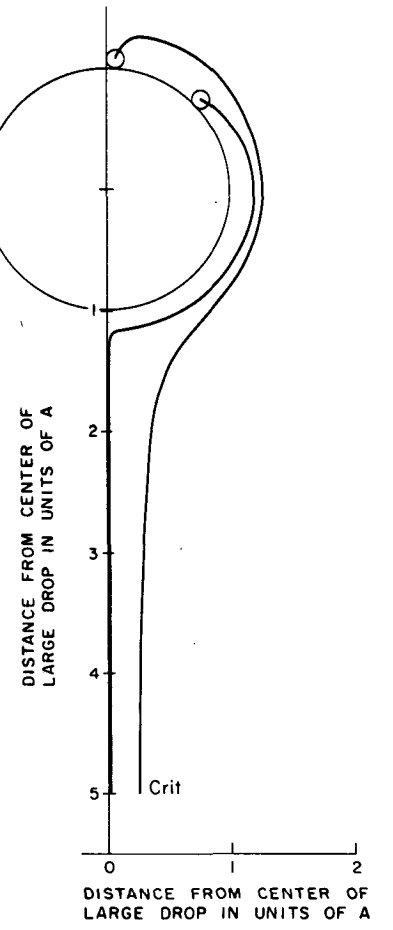

FIG. 11. Trajectories of an $a=2.4$ μm radius drop relative to an $A=40.2$ μm radius drop for the case $q_A=-2=-q_a$, $E_0=-659$ V cm^{-1} and $p=0.06$. The grazing trajectory is labeled Crit.

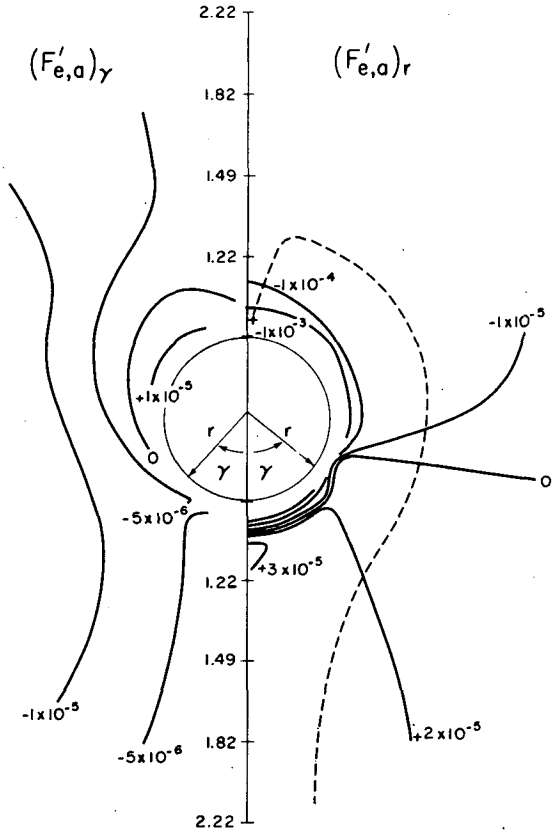

FIG. 12. Radial component (right side) and tangential component (left side) of the nondimensional electrostatic force on the a drop for the case as in Fig. 11. Dashed line is the grazing trajectory.

jectory outside of which no collisions were found to occur.

An explanation of the trajectories is possible by examining the radial and tangential components of the nondimensional electrostatic force, $(F'_{e,a})_r$ and $(F'_{e,a})_\gamma$, respectively, on the a drop.

Fig. 12 displays these two components for $p=0.06$ in a plot in the (r,γ) plane, where γ increases from 0 to π from the vertical axis on each side of the figure. The right-hand side of the figure displays contours (solid lines) of equal nondimensional electrostatic force along the line of centers of the two drops which the a drop would experience if its center was at a given orientation to the A drop. Positive values of $(F'_{e,a})_r$ represent an electrostatic force tending to separate the drops along the line of centers, whereas negative values represent a force tending to bring the drops together. The dashed line represents the grazing trajectory of a 2.4 μm drop. The left-hand side of the figure similarly displays contours of equal nondimensional electrostatic force in a direction tangential to the A drop, with γ defined as shown. Positive (negative) values of $(F'_{e,a})_\gamma$ represent an electrostatic force tending to move the a drop toward increasing (decreasing) values of γ.

It becomes apparent in examining $(F'_{e,a})_r$ that the a drop spends the greater part of its trajectory in a region where it is being electrostatically forced away from the A drop. This results from the action of the external electric field on the charge distributions on each of the drops. It is interesting to note that the region where mutually attractive forces occur at all angles γ due solely to interactions of the charge distributions on each drop is very narrow. Therefore, front collisions are effectively prevented. However, since the a drop has relatively little inertia for $p<0.1$, it may still collide with the rear of the A drop through action of the electrostatic forces tending to bring the drops together at angles $\gamma \gtrsim 80°$.

As the a drop size further increases, E eventually decreases to zero for $A=40.2$ μm, as p approaches 0.1. This occurs since the a drop's inertia increases at a rate proportional to its mass, i.e., as a^3, whereas the electrostatic force on the a drop increases as a^2. Further, as is illustrated by curves 2a and 2b in Fig. 8, the initial relative velocity of the drops is

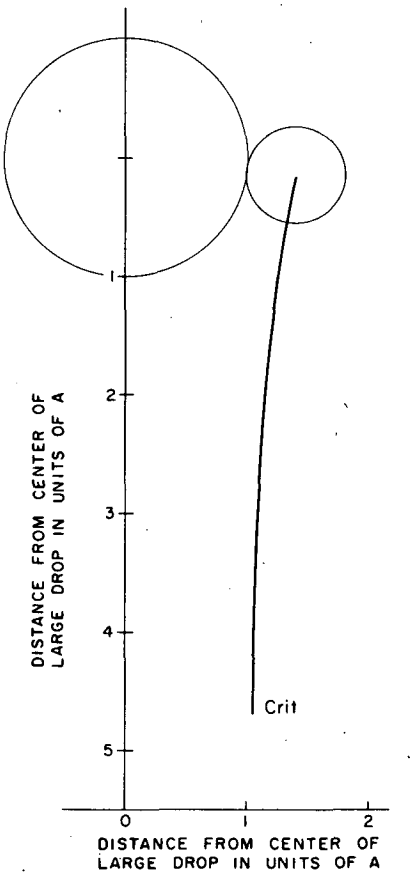

FIG. 13. Grazing trajectory of an $a=11.5$ μm radius drop relative to an $A=40.2$ μm radius drop for the case $q_A=-2=-q_a$, $E_0=-659$ V cm^{-1} and $p=0.286$.

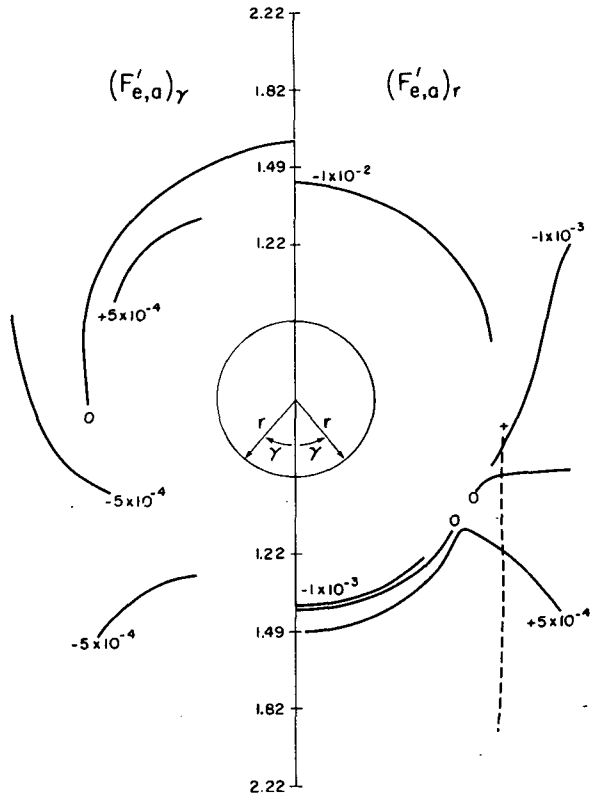

FIG. 14. Radial component (right side) and tangential component (left side) of the nondimensional electrostatic force on the a drop for the case as in Fig. 13. Dashed line is the grazing trajectory.

quite large causing short interaction times. Therefore, the drop has too little inertia to penetrate the "electrostatic force barrier" in front of the A drop, but has too much inertia to allow the relatively weak electrostatic forces in the rear of the A drop to cause a collision.

As the p ratio reaches more intermediate values, the a drop gains enough inertia to break through the slowly increasing "electrostatic barrier" in front of the A drop and collide with it. Rear collisions also occur since the a drop has gained sufficient inertia to cross the hydrodynamic streamlines around the A drop to remain sufficiently close to it even if it just misses collision with the front. However, continued increase in a drop size with persisting short interaction times eventually terminates further rear collisions. This is illustrated by Figs. 13 and 14 for $a=11.5$ μm ($p=0.286$).

Again referring to Fig. 8, as p increases past 0.3 for the 40.2 μm collector the initial relative velocity of the drops has decreased sufficiently to cause a steep rise in the interaction time. This simultaneously allows the increasing electrostatic forces to act over progressively longer periods of time to effectively reestablish the barrier in front of the A drop. As p approaches 0.7 a region of zero collision efficiency results. Only after the interaction time has become sufficiently long with further increase in p do the electrostatic forces behind the A drop act again to force a collision. This is illustrated by Figs. 15 and 16 for $a=28.2$ μm ($p=0.701$).

In the discussion above, the contribution of $(F'_{e,a})_\gamma$ has been neglected. Its magnitude is generally less than half that of $(F'_{e,a})_r$ and therefore contributes only in a minor way to the overall results. This same conclusion also applies to $(F'_{e,A})_\gamma$. Furthermore, the nondimensional electrostatic force component $(F'_{e,A})_r$ is dominated by the action of the external electric field on the charge carried by the A drop. Therefore, its magnitude is relatively insensitive to variation with p. Its contribution to the relative motion of the two drops was found to be in the same direction as that of $(F'_{e,a})_r$.

On the basis of the above discussion it is possible to generalize the results of 40.2 μm drop case to the other collector drop sizes considered. Referring again

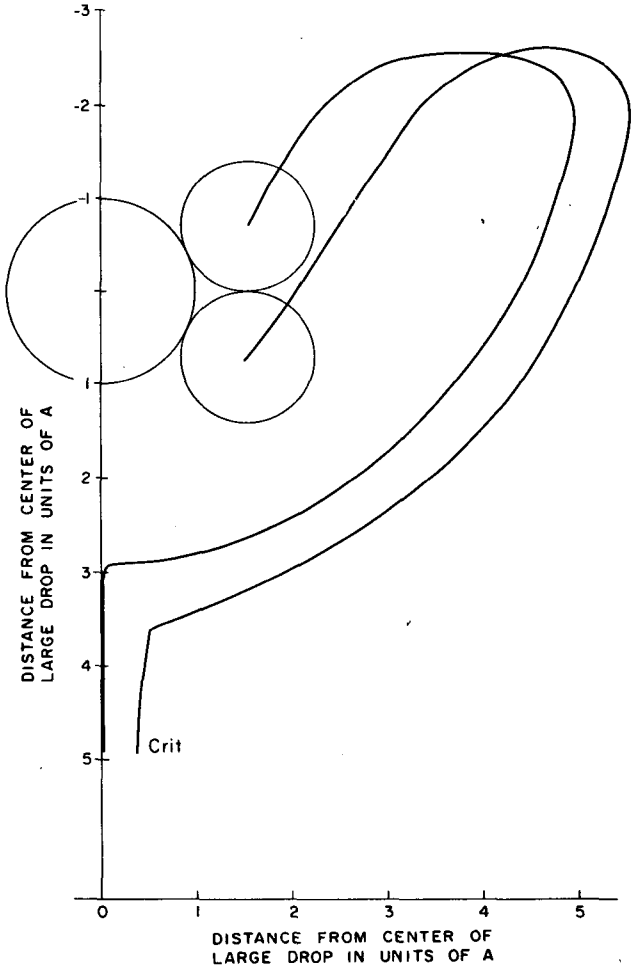

FIG. 15. Trajectories of an $a=28.2$ μm radius drop relative to an $A=40.2$ μm radius drop for the case $q_A=-2=-q_a$, $E_0=-659$ V cm^{-1} and $p=0.701$. The grazing trajectory is labeled Crit.

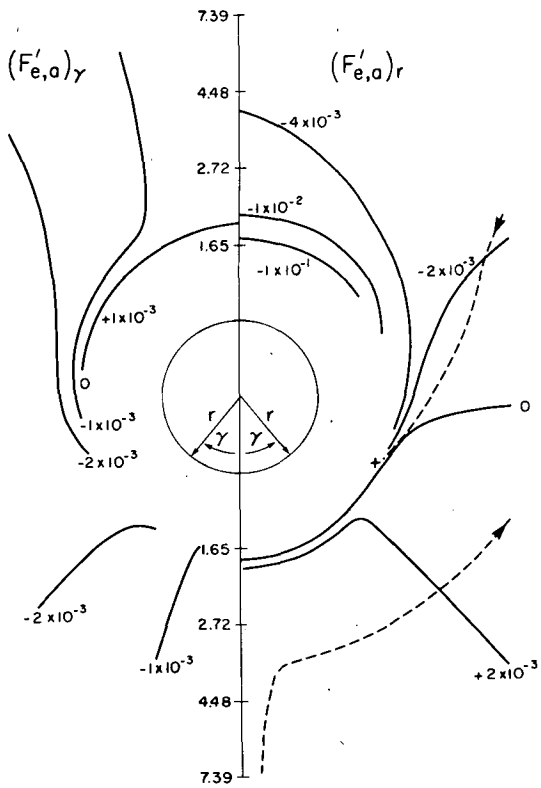

FIG. 16. Radial component (right side) and tangential component (left side) of the nondimensional electrostatic force on the a drop for the case as in Fig. 15. Dashed line is the grazing trajectory.

to Figs. 9 and 10 it is seen that F_{Front} generally increases with increasing A-drop radius, whereas E_{Rear} generally decreases. This is readily understandable by examining Eqs. (1) and (2). As A increases, so does its terminal velocity $V_{\infty,A}$ (see Table 1). Therefore, the overall magnitude of $\mathbf{F}'_{e,a}$ and $\mathbf{F}'_{e,A}$ decreases, while maintaining direction, reducing the "electrostatic barrier" to front collisions. Further, a plot of E_{Front} and E_{Rear} for high external electric field values examined shows the same general trends as Figs. 9 and 10, and also shows that E_{Rear} typically increases as E_0 increases. This is also understandable from Eqs. (1) and (2), since an increase in E_0 results in an increase in the overall magnitude of $\mathbf{F}'_{e,A}$.

In summary, the present results for a negatively charged A drop and a positively charged a drop interacting in the presence of a downward pointing electric field demonstrate that the electrostatic forces are responsible for determining the shape of the collision efficiency curves. The hydrodynamic flow interactions, in this case, are of secondary importance. In contrast, the collision efficiencies derived for the electrostatic configurations considered by Schlamp *et al.* (1976) [who assumed either a positively charged A drop and a negatively charged a drop interacting in the presence or absence of a downward-pointing electric field, or uncharged drops interacting in a downward field] are controlled by the hydrodynamic interaction of the flow fields around each drop. The electrostatic forces, on the other hand, play an important, but secondary role in that they enhance the value of the collision efficiency but appear not to change the basic shapes of the collision efficiency curves.

Acknowledgments. Three of the authors (RJS, SNG and HRP) are indebted to the Atmospheric Research Section of the National Science Foundation for providing funds under Grant DES 75-09999 which were used for carrying out a portion of the research reported in this article. One of the authors (AEH) is indebted to the Canadian Research Council for providing funds for carrying out some of the numerical computations reported in this article. One of the authors (HRP) also wishes to acknowledge the Von Humboldt Foundation for providing funds in the form of a U.S. Senior Scientist Award to carry out some aspects of this research at the University of Mainz, Germany, during 1977.

REFERENCES

Abbott, C. E., 1975: Charged droplet collision efficiency measurements. *J. Appl. Meteor.*, **14**, 87–90.

Atkinson, W. R., and I. Paluch, 1968: Analytical approximation of numerically determined collision efficiencies of hydrometeors, *J. Geophys. Res.*, **73**, 2035–2048.

Davis, M. H., 1962: The forces between conducting spheres in a uniform electric field. Rand Corp. Publ. RM-2607-1PR, 39 pp.*

——, 1964a: Two charged spherical conductors in a uniform electric field: Forces and field strengths. Rand Corp. Publ. RM-3860-PR, 35 pp.*

——, 1964b: Two charged spherical conductors in a uniform electric field: Forces and field strength. *Quart. J. Mech. Appl. Math.*, **17**, 499–511.

——, 1965: The effect of electric charges and fields on the collision of very small cloud drops. *Proc. Int. Cloud Phys. Conf.*, Meteor. Soc. Japan, Tokyo and Sapporo, 118–120.

——, 1969: Electrostatic field and force on a dielectric sphere near a conducting plane—A note on the application of electrostatic theory to water droplets. *Amer. J. Phys.*, **37**, 26–29.

Krasnogorskaya, N. V., 1965: Investigation of the collision efficiency of cloud particles, *Proc. Int. Conf. Cloud Phys.*, Suppl., Meteor. Soc. Japan, Tokyo, 124–130.

——, and A. I. Neizvestnyy, 1973: Experimental investigations of collision and coalescence efficiencies of charged drops in Stokes flow. *Izv. Atmos. Oceanic Physics*, **9**, 220–225.

LeClair, B. P., A. E. Hamielec and H. R. Pruppacher, 1970: A numerical study of the drag on a sphere at low and intermediate Reynolds numbers. *J. Atmos. Sci.*, **27**, 308–315.

Lindblad, N. R., and R. G. Semonin, 1963: Collision efficiency of cloud droplets in electric fields. *J. Geophys. Res.*, **68**, 1051–1057.

Paluch, I., 1970: Theoretical collision efficiencies of charged cloud droplets. *J. Geophys. Res.*, **75**, 1633–1640.

Plumlee, H. R., and R. G. Semonin, 1965: Cloud droplet collision efficiency in electric fields. *Tellus*, **17**, 356–364.

* Available from Rand Corporation, 1700 Main St., Santa Monica, CA 90406.

Proudman, I., and J. R. A. Pearson, 1957: Expansion at small Reynolds numbers for the flow past a sphere and a circular cylinder. *J. Fluid Mech.*, **2**, 237–262.

Sartor, J. D., 1960: Some electrostatic cloud droplet collision efficiencies. *J. Geophys. Res.*, **65**, 1953–1957.

——, 1970: Accretion rates of cloud drops, raindrops, and small hail in mature thunderstorms. *J. Geophys. Res.*, **75**, 7547–7558.

Schlamp, R. J., S. N. Grover, H. R. Pruppacher, and A. E. Hamielec, 1976: A numerical investigation of the effect of electric charges and vertical external electric fields on the collision efficiency of cloud drops. *J. Atmos. Sci.*, **33**, 1747–1755.

Semonin, R. G., and H. R. Plumlee, 1966: Collision efficiency of charged cloud droplets in electric fields. *J. Geophys. Res.*, **71**, 4271–4278.

Takahashi, T., 1972: Electric charge of cloud drops and drizzle drops in warm clouds along the Mauna Loa-Mauna Kea Saddle Road of Hawaii Island. *J. Geophys. Res.*, **77**, 3869–3878.

——, 1973: Measurement of electric charge on cloud drops, drizzle drops and raindrops. *Rev. Geophys. Space Phys.*, **11**, 903–924.